IEEE Access
Multidisciplinary | Rapid Review | Open Access Journal

Received January 5, 2020, accepted January 27, 2020, date of publication February 18, 2020, date of current version March 3, 2020.

Digital Object Identifier 10.1109/ACCESS.2020.2974855

Design and Control of an Underwater Launch System

CHRISTIAN CORWEL, GEORGE ZOGHBI, STEVAN WEBB, AND ABHISHEK DUTTA, (Member, IEEE)
Electrical and Computer Engineering, University of Connecticut, Mansfield, CT 06268, USA

Corresponding author: Christian Corwel (christian.corwel@uconn.edu)

This work was supported by the US Naval Undersea Warfare Center, Newport, RI, USA.

ABSTRACT The ability to launch, or otherwise deploy, a cylindrical body such as an unmanned vehicle, from an outer tube in an underwater environment continues to be of interest to the marine community. Applications of such technologies include the use of small unmanned underwater vehicles (UUV's) deployed from deep ocean craft to support oil exploration efforts or inspection of damaged infrastructure. Historically, these payloads are deployed from their containment tube through the use of a water slug generated from a pump which pushes the vehicle into the open ocean environment.The objectives of this project are to identify and demonstrate a method to launch a cylindrical body from the launch tube utilizing an electromagnetic scheme. It was found that the solenoid coil launching mechanism was the most effective for an underwater launcher. A design was created, modeled in simulations, and finally built and tested to prove its validity. It was found that the solenoid coil launcher could effectively expel a payload with ample exit velocity, low noise, and could be reloaded several times within a minute.

INDEX TERMS Robotics, underwater, electromagnetics.

I. INTRODUCTION

The expulsion of an underwater object from a host has been a topic of research since the first submersible watercraft were constructed. Currently, one of the more popular designs involves pumping water behind the projectile to launch it using the force of the water slug [1]. This design is tried and true, however changes can be made to the overall system that can improve energy efficiency and overall reliability. Pumps that are currently used for water slugs are very large, heavy, loud, and inefficient. In an application such as a submarine, space, weight, and power are all very important factors. For stealth purposes, noise is also crucial, so being able to launch a UUV with little to no noise can be very useful. The technology used for undersea launchers has remained largely unchanged since the 1970s. While these pump designs have been rigorously analyzed and marginally improved over several decades, they can only be expanded upon to a certain point. They do offer some benefits, such as being able to move several thousand gallons of water in under a minute, but the design has run its course. The goal of this paper is to explore different electromagnetic propulsion methods, create an effective design, thoroughly model said design, and finally build and physically test the launch system for validation. While electromagnetic launchers have steadily gained popularity for dry applications, there are exceedingly few designs for electromagnetic launchers in underwater applications. Thus this design will be one of the first of its kind, and will accurately model the capabilities of an electromagnetic underwater launch system.

One possible propulsion method is closely related to the already established EMAL system. EMAL stands for Electromagnetic Aircraft Launch system, and is being implemented on aircraft carriers throughout the U.S. Navy. These systems are much more impressive than current steam catapults, resulting in higher launch capability, reduced weight, volume, and maintenance. They operate by having two massive stators run in parallel down the deck of an aircraft carrier. There is then a carriage placed on a track between the stators that attaches to the aircraft via a detachable hook. The carriage contains highly sensitive magnets, so once current is applied to the stators, the respective electromagnetic force propels the carriage, and therefore causes the aircraft to launch [2]. This may require more housing space than other launching methods, but the EMAL can attain a velocity of 100m/s and launch as quickly as every 50 seconds [3], making it a

The associate editor coordinating the review of this manuscript and approving it for publication was Xiwang Dong.

viable option if a high velocity launch is required. This would also require the design of a detachable hook assembly for launching, which would add significant time to the design phase and give the system a possible source of failure.

Another possible method of propulsion would be magneto-hydrodynamic (MHD) propulsion. This would essentially be an electromagnetic pump which would induce MHD propulsion by using a voltage source to maintain an electric potential between two oppositely polarized electrodes, inducing a Lorentz force in the water between them [4]. The construction for this method could involve one, or multiple, thrusters in the shape of smooth nozzles, each wrapped in magnetic coils. When current is passed through these coils, water is pumped perpendicular to both the current and induced magnetic field, creating a forward thrust [5]. This thrust is a combination of both the water moving through the channel, as well as the pressure increase in the channel creating a pressure differential [6]. This approach would have many advantages. Due to the fact that it has no moving parts, it would be silent, reliable, and easy to maintain [7]. It would also utilize salt water's salinity. Because salt is an electrolyte, the water's conductivity increases, and therefore its ability to be affected by electric and magnetic fields.

A more basic approach to this situation is to use a simple underwater vehicle launcher system. Currently many designs use telescopic cylinders or pneumatic devices to expel payloads from the launch tube [8]. Electromagnetic principles can also be applied in order to launch these fully submersed payloads. There are many ways to apply this type of design, some of which can be adapted from existing electromagnetic torpedo systems. One system is comprised of a sea chamber that takes in water from the surrounding environment. A pump then provides a Lorentz force to the seawater behind the payload, forcing it out of the tube [9]. This system is fairly simple due to the seawater being used for a launch, but requires a large storage tank connected to the tube. A similar system uses an electromagnetic pump to introduce pressure equalized liquid into the launching tube, which is then coupled to force the projectile out of the launch tube [10]. Another torpedo system also uses seawater to propel the package, but uses electromagnetic force instead of any pneumatic pressure from a pump in order to exert force on the seawater [11]. All of these systems would require a large connecting storage tank for the water, greatly increasing material, weight, and size constraints.

A solenoid is another design which can be utilized effectively. This system would be comprised of a cylinder wrapped with a large coil to induce a magnetic field on the projectile in order to fire it. This system requires a large amount of power, but has the advantage of being more reliable and requiring less maintenance than current propulsion systems [12]. Like some of the other systems described, an armature can be utilized so that the projectile does not have to be conducting, which adds versatility to the device allowing many different payloads to be launched using the same system. This system utilizes pulsing waves to create the forces necessary for projectile motion [13]. This adds some complexity over other designs, but is still a viable option for the team to move forward with.

Railguns are simplistic in design, but are very powerful and are a reliable propulsion method. Utilizing two long rails, with a moving armature in between and in contact with both of them, a current is induced and the resulting Lorentz force precipitating from the armature is used to propel a projectile out of the barrel [14]. Various designs have different applications of the armature, sometimes the armature is used to push a non-conductive projectile, and other designs have the armature as the projectile, allowing it to leave the barrel [15]. Either design should be suitable for the application, as this device that will not be traveling at more than several feet per second, so there should be no considerable stress on the armature as a result of repeated use to push the main projectile.

Railguns have several advantages over other electromagnetic designs. Unlike inductive electromagnetic accelerators, they do not require complex circuitry including high voltage transformers, specialized switching and timing circuits, and high voltage capacitors [16]. The main principle of the design is to use DC current to provide all of the forces required to launch the projectile. In order to increase the efficiency of the design, an inductor charging system can be used in place of pulsed alternators or bulky capacitors to power the railgun [17]. This design would also minimize the size of the system and could use batteries to power the system as well. Utilizing a railgun with inductive storage would benefit from the high energy density of the inductor system along with a low cost to build compared to similarly specced large capacitor systems [18].

For this application, waterproofing of electrical components was also researched. It was found that a common method of waterproofing involves placing PCB components into a waterproof case that wires are then ran out of [19].This protects all electrical components from water exposure while still allowing electrical contacts underwater. Due to the underwater nature of the project, all electrical terminals will also need to be waterproofed. This is often done by applying a waterproof resin to the exposed terminals [20]. Both of these techniques will be useful in shielding the electrical components from moisture.

Overall, there are several design choices to move forward with. Each has its own advantages and disadvantages, though the one best suited for proving the concept of underwater electromagnetic propulsion will be chosen. The next step is to pick a design, start hand calculations, and run computer analysis in preparation to develop a physical prototype.

II. SYSTEM REQUIREMENTS AND CONCEPTUAL DESIGN

A. SYSTEM REQUIREMENTS

The system shall be designed from the following parameters. Primarily, the system must be able to launch a payload from an outer tube using an electromagnetic scheme.

The launching system must be re-loadable, and shall be able to expel payloads multiple times within a minute. No specific exit velocity has been established, but the payload must be able to fully clear the tube during the launching process.

The system must be functional when completely submerged in water. This will require the waterproofing of all electrical components, or any other parts of the system that may be susceptible to damage from moisture. Long term corrosion from underwater usage is not being evaluated in this design.

There are no weight or material requirements for this system, but the launching apparatus must conform to a cylindrical shape. Given the literature review of the several different launch systems, an analysis was performed and each design was ranked on several different design parameters. Through this analysis, the best core design to take a baseline from could be chosen.

The first attribute is simplicity of design; from a reliability and continued maintenance perspective, the design of the launcher should be a medium between simplistic and effective. The greater the simplicity of each respective launch system, the more effectively it could be modified to suit an underwater application. The second is the simplicity of the circuit. The control circuit for any launcher is the metaphorical brain of the entire unit, and must function as expected while being easy to debug for errors. The third is the size and the weight constraints. On any ship both size and weight are very important considerations, so the lighter and smaller the system is, the higher its score. The fourth is the power required to operate such a system. Some launch systems require charging power from the host for several minutes, crippling the host's other functions during that time period. The more efficient the system is when it comes to power usage, the better. Design size flexibility reflects the launcher's ability to fire differently sized objects, important for a prototype design such as this. Reliability determines the likelihood a system functions as intended for each and every use. Exit velocity represents how fast the system can expel a payload. In this case a high exit velocity is not a requirement, but exit velocity is important to ensure that the payload will fully clear the tube upon ejection. The last attribute is the cost effectiveness of the system. If a system is too expensive to be practical, its design will likely never make it through the prototype stage, so the better results for a lower cost is an important factor. Each of the designs were given a score of 1-5 in the discussed areas, and the final design was chosen from these scores:

Given these requirements, there are several possible choices of design. The EMAL system was considered for this application, but ultimately denied because of several drawbacks in the design that would make it difficult to meet the requirements. This design would require a carriage to transport the payload down the tube and then finally launch it. For such a small scale design this would be exceedingly difficult, and the carriage would either need to be mounted inside or below the tube. This combined with the need for stators would make the design extremely inefficient for the small scale being used. Such considerations led to low scores for simplicity, size/weight constraints, and cost effectiveness. The next design considered was magneto-hydrodynamic (MHD) propulsion. This would use a type of electromagnetic pump to provide a force on water within the tube that would then launch the payload. This often requires an external storage tank to house the water before launch, as well as a commercial pump to provide the force. It would also require complex circuitry including motor drivers, pump controls, and result in a low exit velocity. Thus the MHD design scored low in simplicity, power and exit velocity, leading to it being removed from the list of possible designs. The final two designs considered were the railgun design and the coil gun based launching system. The railgun functions similarly to the EMAL, with two stators that provide force on an armature to accelerate a payload. This design has the potential to give the highest exit velocity, with decently high scores for simplicity. A large drawback of this design is that it is prone to arcing, which dampens the reliability and could have increased frequency in an underwater medium. The need for two stators also lowers the score of the size and weight requirements, leading to a total score of 30 for the railgun approach.

TABLE 1. Design comparison table.

	Railgun	Coil Gun	EMAL	MHD
Requirements (Score 1-5)	**Score**	**Score**	**Score**	**Score**
Simplicity of Design	4	5	2	1
Simplicity of Circuit	4	5	3	1
Size/Weight Constraints	3	4	3	3
Power Required	3	3	2	2
Design Size Flexibility	4	4	3	5
Reliability	3	5	3	4
Exit Velocity	5	4	4	2
Cost Effectiveness	4	5	2	4
Total Score	30	**35**	22	22

After careful deliberation and comparing of the designs above, it was decided that an electromagnetic coil gun based launching system would be the most effective for this application. This design was chosen because of its relative simplicity and cost effectiveness. There are no moving parts in the design except for the payload itself, meaning a mechanical failure is highly unlikely. The design also consists of a simple charging circuit centered on very few components. This greatly increases reliability because there are less possible points of failure. This design is also exceedingly cheap for the results that are expected, it is comprised of inexpensive circuit components that could easily be replaced in the event of a failure. This design is also the perfect basis for the use of an outer tube, because the whole system can be contained to a circuit box and the launch tube itself, which will have the coils wrapped around it. The ''coilgun'' is a simple concept that operates via the core principles of electromagnetism. It will not require any kind of stators or launch tube modification past the winding of coils around the tube.

B. CONCEPTUAL DESIGN

The solenoid launcher will be designed to ensure the successful launch of the chosen projectile in an underwater environment. This will require a force that can counteract the pressure of the water and the friction. The system will be comprised of the coil wound around a dielectric tube, a capacitor bank for power, and a system of relays with a power supply to charge the capacitors to launch the projectile using an armature. This will ensure launching flexibility for several different sized payloads, a simple representation of the system is shown below:

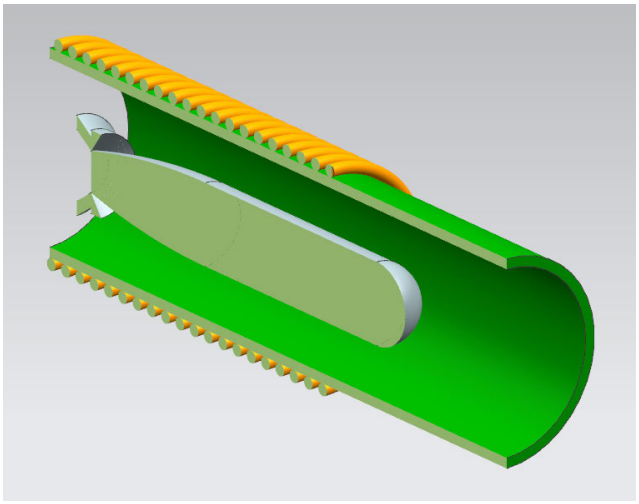

FIGURE 1. 3D representation of the coil launcher system.

The main premise for the coil gun is its ability to generate a magnetic field, which can be utilized to either launch a magnetic projectile, or accelerate any object, regardless of its magnetic properties, placed inside using an armature. The coil accomplishes this via Faraday's law of induction:

$$\epsilon = -N\frac{d\Phi_B}{dt} \tag{1}$$

Here, ϵ is the electromotive force and Φ_B is the magnetic flux through one loop of wire. Thus, the electromotive force will be parallel to the magnetic field generated in the solenoid. This concept can be applied to the solenoid design to create a force that will propel a ferromagnetic object through the coil by simply inducing a current through it:

The strength of this magnetic field is dependent on several factors:

$$B = \mu_o\frac{N}{l}I \tag{2}$$

The value of μ_o is equal to the relative magnetic permeability inside the coil compared to in vacuum. In this case, the coil will be underwater, but the value will still remain 1 as water's relative permeability is the same as in air. The value of N is the number of turns in the coil, the value of l is its length. The third variable, I, is the current running through the coil. These values are easy to modify as well

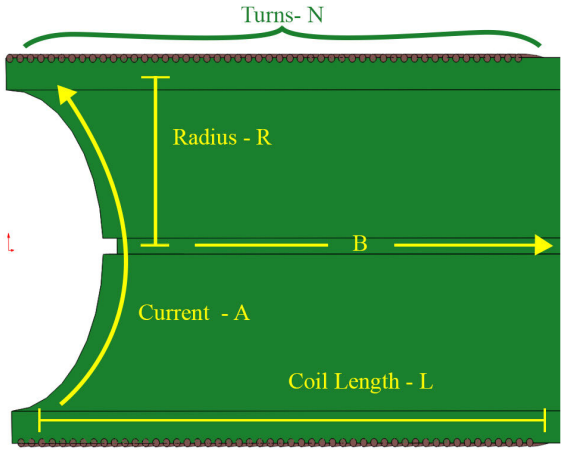

FIGURE 2. Magnetic field induced by current in a solenoid.

for a specified parameter. For example, simply adding more turns of coil will increase the magnitude of the magnetic field. Thus, equation 2 can solve for launching any projectile for any exit velocity or travel distance.

The value for the magnetic field, B, can be related to the exit velocity of the projectile in terms of the force exerted by the magnetic field:

$$F = \frac{B^2A}{2\mu_o} \tag{3}$$

Here, B is the value in Teslas for the magnetic field calculated in equation 1. The value of A is the cross-sectional area of the core, and μ_o is the magnetic permeability in vacuum (4πE-7). The design excels here as well because simply varying the magnitude of the magnetic field allows for variable launches with different payloads.

In order for this design to function properly as stated above, a charging circuit must be implemented. This circuit will be designed to give the system the high energy pulse that is required. The most critical circuit component will be a capacitor bank. This will undergo a charging cycle from a dedicated power supply, and then quickly discharge into the coil, giving the system the energy it needs to deliver the payload. The bank shall be comprised of several capacitors in parallel, to increase energy storage and in turn launcher effectiveness. The circuit will also require a switch, to change the capacitor bank from charging mode to discharging modes. This can be accomplished by a multitude of different transistors or relays. The circuit may also require damping components to prevent the current from oscillating within the solenoid. Finally a trigger mechanism must be added in order to initiate the launch, and can be implemented with a standard push button.

III. MODELING AND SIMULATION

Several techniques were applied to the analysis of the system. Hand calculations were completed using equations 2-5 with realistic design values to assign a basis for the simulations. In order to obtain the current used in magnetic field and force

equations, circuit analysis was performed on the charging circuit design, which is shown below in figure 3.

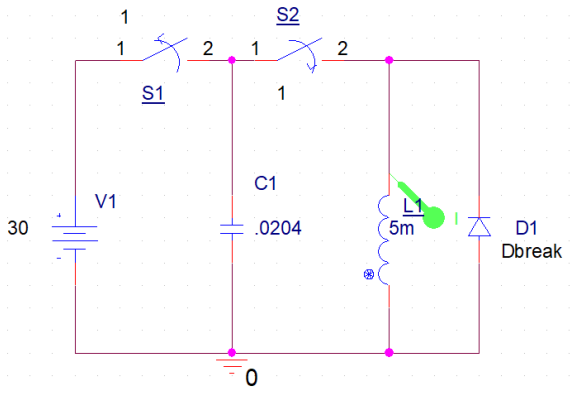

FIGURE 3. Cadence representation of charging circuit.

This circuit consists of a DC voltage source stable at 30V, connected through a switch S1 to a capacitor bank with a nominal value of .0204F. This bank is then connected through a second switch S2 to an inductor which represents the solenoid of the launch system. A rectifier diode was also placed in parallel with the inductor, to serve as a dampener for the circuit. By equating the energy stored in the capacitor to the energy stored in the inductor during the operation of the circuit, the following equation can be derived for maximum current through the inductor. The full derivation is available in appendix.

$$I = \sqrt{\frac{1}{LC}Q^2} \tag{4}$$

In equation 4, L is the inductance of the solenoid, C is the capacitance of the capacitors in the circuit providing the voltage and current, and Q is the charge of the capacitors. The charge of the capacitors is easily found by multiplying capacitance by voltage across the capacitors. The important parameter in this equation with respect to the solenoid is the inductance L. Inductance of a long solenoid is given by the following equation:

$$L = \frac{N^2 \mu_o A}{l} \tag{5}$$

In this equation N denotes the number of turns of wire, A is the cross sectional area of the the solenoid, and l is the length of the solenoid. Thus by manipulating the size of the solenoid, a different inductance can be achieved, therefore altering the current within the circuit. As shown in equation 5, as inductance increases, current decreases, so the solenoid should be kept at a fairly low inductance for best results. Once the solenoid is constructed L will remain constant, therefore capacitance will become the most important parameter that can alter current. The relationship between capacitance and current is direct, therefore increasing the capacitance within the bank will increase current and in turn increase the intensity of the magnetic field within the solenoid. Applying this to equations 2 and 5, the effect of capacitance on the magnetic field can be derived. This relation is shown in figure 4:

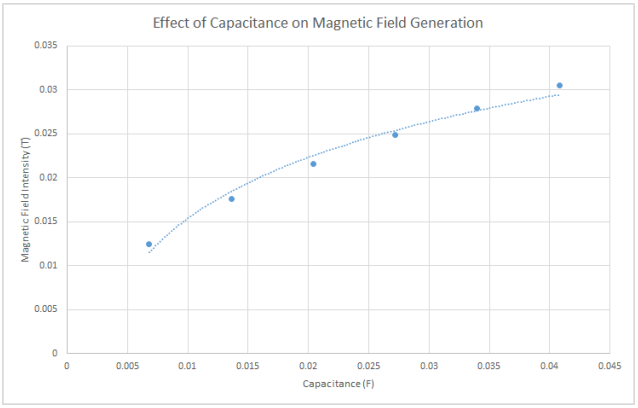

FIGURE 4. Plot of magnetic field vs capacitance.

As this plot shows, one can steadily increase the capacitance in order to achieve a greater force on the object within the coil. Thus the circuit can be kept at a relatively low voltage, meaning less power will be dissipated overall. It should be noted that the increase in capacitance leads to a greater time constant and therefore a longer discharge period for the capacitors. But this impact is minimal and the discharge period will still be within the desired range to prevent the payload from being pulled back into the coil.

To model the charging circuit behavior and output, Cadence Capture CIS 17.2 was used. For the simulations S1 was set to open at one second, disconnecting the capacitors from the DC charging source. S2 was then set to close at 1 second, immediately connecting the capacitor bank to the inductor. This allowed the circuit to function as two separate halves, with the charging phase occurring from 0 to 1 seconds, and the discharging phase beginning at 1 second. Once the discharging phase was entered, the capacitors provided the inductor with a pulse of high current for a short period of time. This would in turn produce a high magnetic field within the solenoid, theoretically pulling the payload through the coils. Current probes were placed on the inductor, and results reflect the current traveling through the coil. Initially the circuit was tested without the use of a rectifier diode, this simulation is shown below in figure 5.

Using the simple inductor model, a very large oscillation was observed in the current through the inductor. Figure 5 shows this oscillation, with the current through the inductor peaking at roughly 60 Amperes and then dropping to -60 Amperes before starting to decay over time. This peak current is equivalent to the current calculation done using equation 5 with the same parameter values, but this would cause a serious problem with the operation of the unit. As shown in figure 2, the magnetic field direction is dependent on the direction of the current. If the current flows in the negative direction, the resultant magnetic field would then be generated in the opposite direction, towards the back

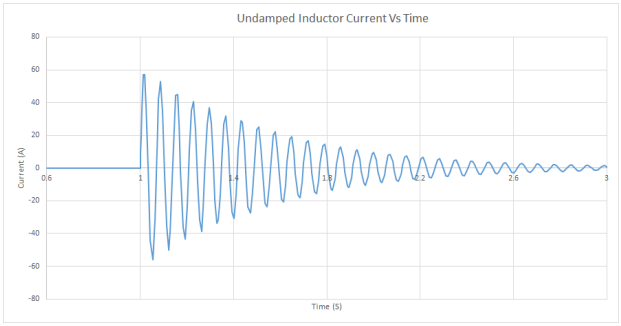

FIGURE 5. Simulation result of initial circuit.

of the tube. This would effectively prevent any object from launching, because it would experience an initial velocity forward, but immediately be pulled back by the oscillating current. Thus a solution had to be implemented to dampen this oscillation, and a rectifier diode was chosen for this purpose. The rectifier diode will cancel oscillation without altering the current that passes through the inductor. This was chosen over components like resistors, which would change the current in the inductor and add more variables to the circuit equations. The damped current through the solenoid is shown below in figure 6.

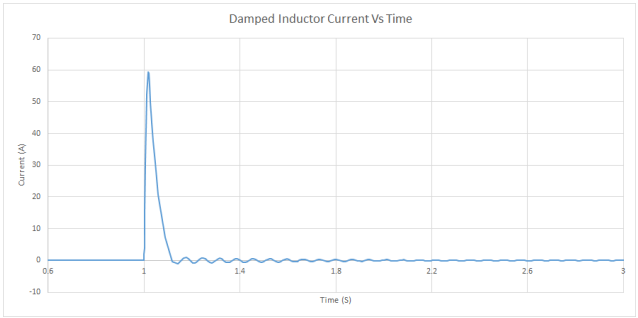

FIGURE 6. Simulation result of damped circuit.

As shown above, the addition of the rectifier diode greatly increases the performance of the circuit without compromising on current magnitude. Equally as important is the width of the primary pulse in seconds. The rectifier diode only slightly increases the pulse width, still keeping it well within desired range of under 150 milliseconds. The refined circuit also has an oscillation of less than 5 amperes after the initial peak, meaning any residual magnetic field will be too weak to have an effect on the payload. It is also important to note that when this is physically applied in the prototype stage, the internal resistance of the wire will also help to dampen the current running through the coil, likely resulting in a current slightly lower than that observed in the simulations and a pulse width slightly shorter. With these circuit simulations complete, the components can be selected based on given parameters and the physical circuit constructed.

To simulate the magnetic field within the solenoid, ANSYS Workbench 19.1 was used. A MAXWELL 2D simulation

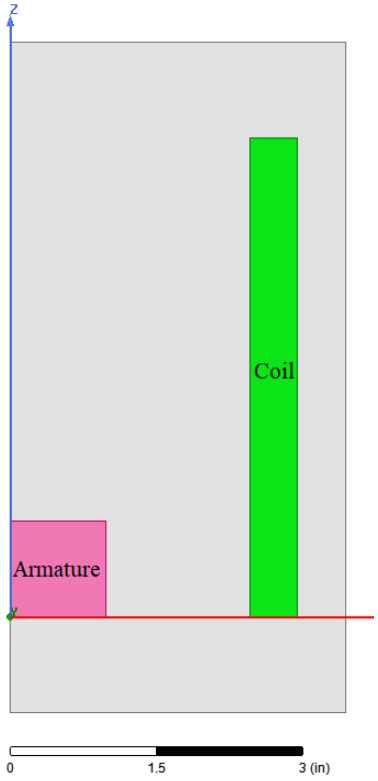

FIGURE 7. Simulation model of the solenoid launcher.

was created to model the system. A 5" long solenoid of $N = 200$ turns with an inner radius of 2.5" and a 1" $\times$ 2" armature of iron were inserted and analysis was performed with 60 Amperes of current flowing through the coil. The MAXWELL environment allows the ability to model a 3D solenoid in a 2D environment for ease of analysis while still maintaining high precision. Figure 7 shows a 2D representation, where the coil and armature are cross sectioned so that they can be thought of as extruding outwards and from the front and back of the screen, and coiling around to the opposite side of the z axis to create cylinders.

In the analysis, a high magnetic field is observed surrounding the armature. It is shown below in figure 8 as the red and yellow area on the edge of the iron armature. This is because of the armature's ferromagnetic properties and how MAXWELL calculates the field. In real world testing, such a high magnetic field on the boundary will not exist. Thus, this force will not have a substantial effect on the movement of the object. The value of the magnetic field inside of the coil is more important and when compared to hand calculations, is substantiated.

As the results show, the value of the magnetic field around the armature is roughly 0.1 Teslas. Inserting this value into equation 3 results in approximately 7.957 newtons on the armature. This value is in line with hand calculations, thus can be used in the modeling for the device as it is refined for the final design.

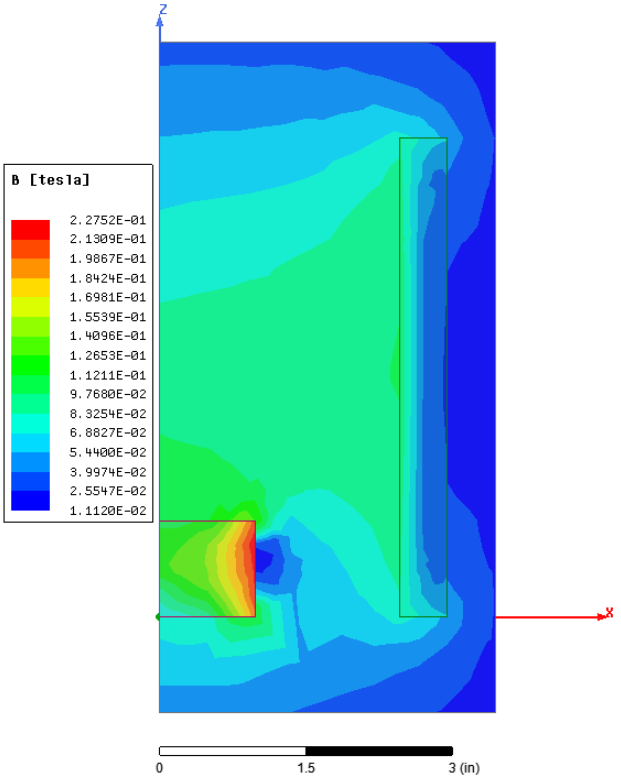

FIGURE 8. Simulation result of the solenoid launcher.

By applying the results from the simulations and using this initial impulse force, the initial velocity can be solved for by using the following derivation:

$$F_i = ma \tag{6}$$

$$v_i = at \tag{7}$$

$$v_i = \frac{F}{m}t \tag{8}$$

where v_i denotes the instantaneous velocity, Fi denotes the impulse force from the magnetic field, m is the mass of the object being launched, and t is the pulse length. After the object experiences this impulse force, the only other force acting on the payload is the drag due to the water pressure and the friction. Using this information, the following derivation for drag can be achieved:

$$F_d = V^2(\frac{1}{2}p)(C_dA_f + C_dA_s) \tag{9}$$

In this equation, V is the instantaneous velocity of the projectile. The density of water, p, is assumed to be 1g/mL. Af and As denote the cross sectional area of the front and sides of the propelled object respectively. C_d denotes the drag coefficient of the object, approximated to be 0.82. The payload itself was assumed to be neutrally buoyant with a mass of .72kg. Due to the complexity of the system of equations and the fact that the forces are always changing, solving analytically for the solution was deemed inefficient. Instead an iterative graphical method was adopted, and the velocity profile is shown below:

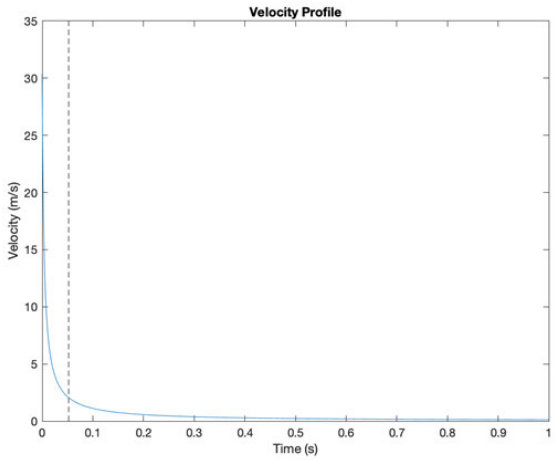

FIGURE 9. Velocity profile of payload.

The dotted line on the plot represents the moment in time when the object fully departs from the tube. With these parameters and the impulse force of 8 newtons, the exit velocity is equal to 2.05 m/s. With this velocity, the payload will fully exit the tube and continue into the underwater environment. Using velocity and iterating over units of time, the distance the payload travels can also be shown graphically:

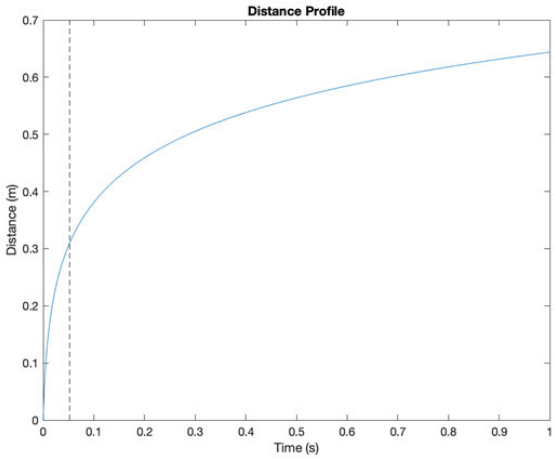

FIGURE 10. Distance profile of payload.

This plot gives a traveling distance of roughly 0.64m after the payload has exited the tube. This fully satisfies the requirement of the payload having to clear the tube on launch. It is likely that the residual momentum may even carry it further, but not a very significant distance, as shown in the plot. It is worth noting that these simulations were ran with a fraction of the available capacitors for the prototype, and that the physical design will likely be able to launch payload further. With these simulations complete and all theories

and equations proven, the first stage prototype can now be designed and constructed.

A. EXAMPLE CALCULATION

This section will serve as a full design example using equations 2-5. This example has the following constant values:

- A solenoid with $N = 200$ turns, 0.127m in length, and a radius of 0.0635m
- A capacitor with a value of .0204F charged to 30V

First the inductance can be solved for with the physical parameters of the coil:

$$L = \frac{N^2 \mu A}{l}$$

$$L = \frac{200^2 * 1.26 \times 10^{-6} \frac{\text{H}}{\text{m}} * 3.17 \times 10^{-3}\,\text{m}^2}{0.127\,\text{m}} = 5.01\,\text{mH}$$

Then using the inductance the current through the solenoid can be solved for:

$$I = \sqrt{\frac{1}{LC} Q^2}$$

$$I = \sqrt{\frac{0.612\,\text{C}^2}{5.01\,\text{mH} * 0.0204\,\text{F}}} = 60.53\,\text{A}$$

With the current, the magnitude of the magnetic field is calculated:

$$B = \mu_o \frac{N}{l} I$$

$$B = 1.26 \times 10^{-6} * \frac{200}{0.127\,\text{m}} * 60.53\,\text{A} = 0.120\,\text{T}$$

This calculation for magnetic field assumes that this is the value in the exact center of the coil whereas in reality the armature resides on the edge of the coil initially, so the magnetic field can be approximated to a lower .1 Teslas. Finally, the force on the armature is calculated:

$$F = \frac{B^2 A}{2\mu_o}$$

$$F = \frac{0.01\,\text{T} * 0.002\,\text{m}}{2 * 1.26 \times 10^{-6}} = 7.96\,\text{N}$$

IV. SUBSYSTEM DESIGN: SIZING AND COMPONENT SELECTION

Several factors were considered in the sizing of the system. One of the most important parameters is the diameter and length of the launch tube, which directly impacts the ability to launch as well as the size of the solenoid. In order to derive the best possible diameter for the tube, behavior of the water within the tube during the launch sequence was observed. ANSYS simulations were performed for fluid dynamics and drag effects. The following plot shows drag effect based on the ratio of D:d, where D is the tube diameter and d is the payload or armature radius.

Given this information, it was decided that the tube diameter ratio would be set at 2.5:1, as the graph shows diminishing returns past this ratio. With a larger ratio, more current would

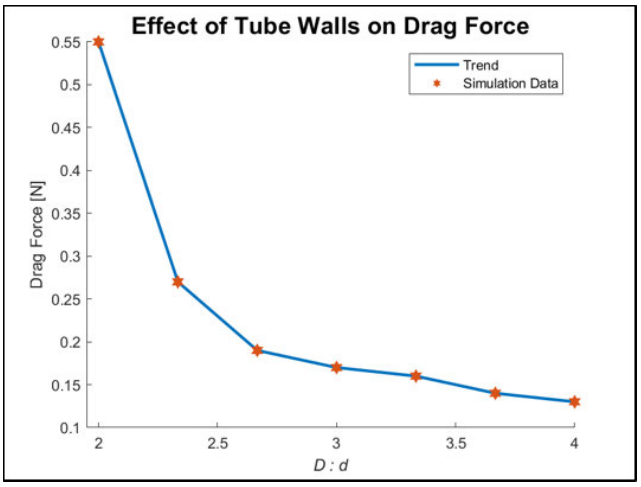

FIGURE 11. Tube diameter vs drag force.

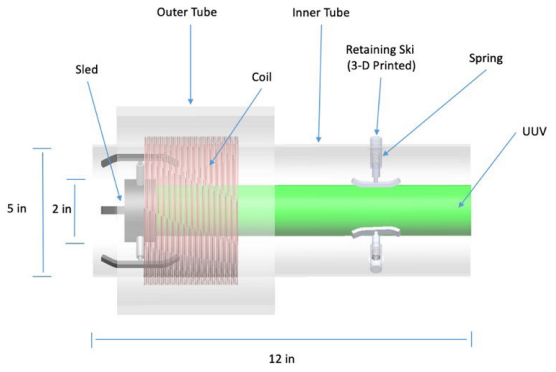

FIGURE 12. Preliminary physical prototype.

be needed to generate the same magnitude of magnetic field over the larger cross-sectional area. This gives a relatively low drag force on the payload during launch, which in turn will give a higher velocity and further launch distance. From this analysis, it was decided that the tube diameter should be set at 5 inches, and the armature diameter set at 2 inches. This gives the desired ratio for optimal drag force reduction. These choices were also chosen based on the strength of the magnetic field within the solenoid. The greater the diameter of the launch tube, the less concentrated the field will be; but this sizing will produce a strong field while also cutting down on drag forces.

Length of the launch tube is not as critical of an aspect. The tube will be longer than the solenoid, which was simulated at 5 inches in length. The tube must also be short enough to allow the payload to fully exit while it still has a substantial velocity. With this criteria, a tube length of 12 inches was proposed for the physical prototype. Mechanical details were also implemented to further the capability of the system. These include an armature connected to sleds that will push the payload, and retaining skis to hold the payload in the center of the tube during the launch. Taking all of these factors into consideration, a model for the prototype is shown below:

It should be noted that this model does not contain any of the circuit components except for the coil. A separate

container will be built to house the rest of the circuitry to isolate them from any contact with water. This box will be designed and constructed after initial lab testing confirms the functionality of the circuit.

Taking this design into consideration, circuit components were selected to maximize the capability of the launcher system. Five components have been specified to meet the specifications for a successful launch: a 30V power supply, switches, capacitors, a rectifying diode, and the coil.

The power supply will be provided by the University of Connecticut, and will be a variable lab grade DC power supply. It is a model 2231A-30-3 DC power supply manufactured by Keithley. This power supply will charge the capacitors in the circuit to a maximum of 30V. The ability to adjust the output voltage of the unit is also important for testing and refining the prototype launch system.

The switch used that will be used in the physical prototype is an electrical relay, model B01N8P5Q50 manufactured by Uxcell. A relay was chosen because it acts as a controllable electrical switch with a higher current rating than manual switches. This particular relay acts is an SPDT switch, where the single pole is connected to the capacitors and the switch can change between contacting the power supply and the solenoid. This relay was chosen because it is rated to 100A, so it will not fail when the current from the capacitors is transferred through it. This particular model contains an LED indicator light, so the switch state can visually be observed. It also requires a bias of 12V in order to switch from one state to the other, and this is done by using the second channel on the DC power supply.

A manual switch was selected to act as a control for applying the 12V bias to the relay. This manual switch will be toggled by the user when the system is ready to fire. This will deliver the 12V bias to the relay, making the relay position change to the discharging configuration and therefore launching the payload. The switch selected for this purpose is a 360-3289-ND SPST switch from the NKK switch company. This component is rated to 6A, which is more than double the maximum current it will see while connecting the relay to the 12V bias.

The capacitors that will be used in the physical prototype are electrolytic capacitors provided by Cornell Dubilier, model number SLPX682M050C7P3. Electrolytic capacitors were chosen because they offer a much higher capacitance than parallel plate capacitors, and are often housed in more durable packages than ceramic devices. The selected units have a capacitance of 6800μ F, as well as a voltage rating of 50V. Therefore they will be able to store a large amount of energy due to the high capacitance, and the 50V voltage rating ensures the capacitors will not be subject to damage during the charging phase. Ten units were ordered to construct a bank to launch the projectile. This gives a maximum possible bank capacitance of 68,000μF, with 30V across each capacitor.

In order to construct the coil, 16Ga magnet wire manufactured by Remington Industries was selected. This is wire coated in enamel that is designed for use in electromagnetic induction systems, so it can be coiled on top of itself without creating a short. A 5 lbs. spool of this wire was selected, which will be sufficient to achieve the target of 200 coil-turns over a length of 5 inches. This product also has a temperature rating of 155C, therefore, it will not be damaged from the heat generated by the high pulse of current.

The final crucial component is a rectifier diode. This diode will function as a short directly to the ground when a forward voltage is applied to it. The inclusion of the diode rectifies and dampens the output, preventing unwanted oscillation within the coil as the projectile travels through it. This component is a model VS-100BGQ100 Schottky Rectifier diode sold by Vishay Intertechnology. This diode has a forward voltage of .82V, so it will switch to the on position and drain current almost immediately after the initial voltage pulse. This diode is also rated to sustain a constant current of 100A, so will handle a high current for a short period of time.

These components are all required for a successful launch of the projectile. Each has been selected for their specific use. The final design may use different components and ratings but they will all be of the same type and design.

A summary of important component ratings are shown below:

TABLE 2. Table of component ratings.

Component	Manufacturer	I (A)	VDC (V)	T (C)
Power Supply	Keithley	3	30	N/A
Switching Relay	Uxcell	100	100	-20∼80
Toggle Switch	NKK Switches	6	30	-30∼85
Capacitors	Cornell Dublier	N/A	50	-40∼85
Magnet Wire	Remington	N/A	N/A	-30∼155
Rectifier Diode	Vishay	100	100	-55∼175

As shown within the table all of the components selected will be able to withstand the stresses applied to them during the physical circuit building and testing. Components with specifically high current and temperature ratings were chosen because of the high pulse of amperage that the circuit will experience during the discharging phase. The circuit will be subjected to a relatively low voltage, well below the component ratings. Therefore voltage tolerance is not a critical design factor for the launcher. With these components selected, the first physical prototype can now be constructed.

V. INTEGRATION: HARDWARE AND SOFTWARE IMPLEMENTATION

An important aspect of this project is the integration of the physical circuit and the launch tube itself. Due to the underwater environment the launcher will reside in, the circuit had to be implemented in a way that would resist any destruction from the surrounding water. The circuit component that must reside directly within the tube is the coil of wire, which will be enclosed in an outer PVC pipe to protect it from the surrounding water. This coil, as stated earlier, will be used to create a magnetic field that propels the armature to launch the UUV. This means that the other circuit components can

be connected to the tube through a conduit that will lead to a box containing all the other circuit components mentioned in Section IV. By containing the circuit in a box outside of the water, the likelihood of part damage from moisture is greatly reduced. This would also simulate having the circuit safely stored within the body of an underwater vehicle, as well as providing a well designed carrying system for all the circuit components so that the system is much less likely to be damaged by transportation. This design concept is shown in the following figure:

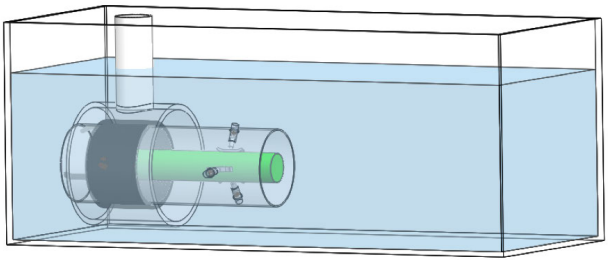

FIGURE 13. Design concept with wire conduit.

As shown in the figure, two wires from the positive and negative ends of the coil will be run through PVC pipe from the tube up, and then into a box (not pictured). The junction between this conduit and the launch tube will be sealed and waterproofed to prevent any moisture inside the coil or conduit. In theory the copper enameled wire that makes up the coil would be able to withstand being in an underwater environment, but this waterproofing redundancy was added in order to increase the reliability of the system overall. All of the physical parts inside the launch tube, such as the armature and retaining skis, will consist of material that will be unaffected by the water within the tube, such as steel, iron, or 3D printed plastics. This will successfully integrate the physical launch tube itself with the circuit, using a method that will keep all electrical components safe from environmental effects.

All individual components must also be integrated to create the final circuit contained within the box. This requires the wiring of the power supply, capacitor bank, rectifier diode, multiple switches, and the electromechanical relay used to switch the circuit into firing mode. The physical circuit shall be wired slightly differently than the Cadence model shown in figure 3. It will function on the basis of the user implementing two separate switches to first charge the capacitors, and then engage the relay. The first switch, labeled S1 in figure 3 will be originally in the open configuration, and then moved to the closed position by the operator to charge the capacitor bank. Once this switch is engaged the voltage bias from the power supply will charge the capacitor bank and the launcher will be primed and ready to fire.

The capacitor bank will consist of several capacitors wired in parallel stored safely within the circuit box. Once the bank has been charged, the operator will then move the switch back to the open position, to disconnect the power supply and prevent any of the current from traveling back to the power supply and damaging it. The bank shall be comprised of multiple packs of 5 capacitors each, as shown below:

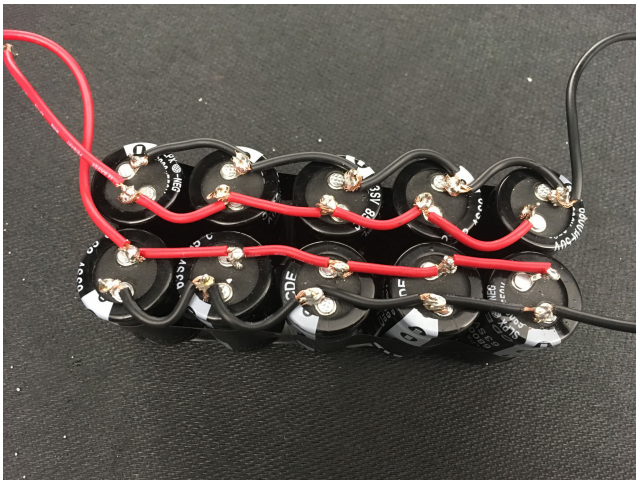

FIGURE 14. Capacitor bank selective wiring.

These capacitors will be wired specifically in this configuration so that if one capacitor fails it will not compromise the integrity of the entire bank. In the event of multiple failures it will also be easy to switch out an entire group of capacitors for a fresh set. This also allows for sets of 5 more capacitors to be easily added if more power is required. Theoretically any number of capacitors can be added to the bank, but the higher the capacitance of the bank, the longer it will take to completely discharge.

The second switch will be used to control the electromechanical relay denoted as S2 in the model, applying a 12V bias to the relay causing it to move from an open position to a closed position. The operator will flip this switch to close it and launch the projectile after completing the charging phase detailed above. For an extra step of verification the relay contains an LED indicator light which turns on when the switch is closed, so the operator can visually check the relay to make sure it engages properly. All of the switches as well as the relay will be mounted on the top of the box, for use by the operator. This will allow for a very rapid use of the launch system by any trained operator.

The power supply will be wired into the box, with the positive wire being connected to the first switch, and the ground wire being connected to the capacitor bank. During initial testing, the source of voltage will be the variable lab grade DC power supply described in Section IV. This method was chosen because it allows for a consistent voltage to be delivered to the circuit and is not resource intensive. Once a consistent and desired exit velocity is achieved, the voltage source will be changed to a series of 9 Volt batteries. This design choice allows for greater portability, which will be important for both further testing and demonstrating outside of the lab.

By integrating each of these components and wiring them as stated above, the system will function effectively and be ready for testing. All physical construction of the launcher system was done in the electrical engineering laboratories of the University of Connecticut.

VI. PERFORMANCE VERIFICATION AND VALIDATION

Several tests were performed on the system after its initial construction. For the purpose of this experiment, multiple armature designs were considered, and dry and wet-testing were completed for all of them.

The first full tube and coil prototype was built to the exact specifications established previously, and is shown below:

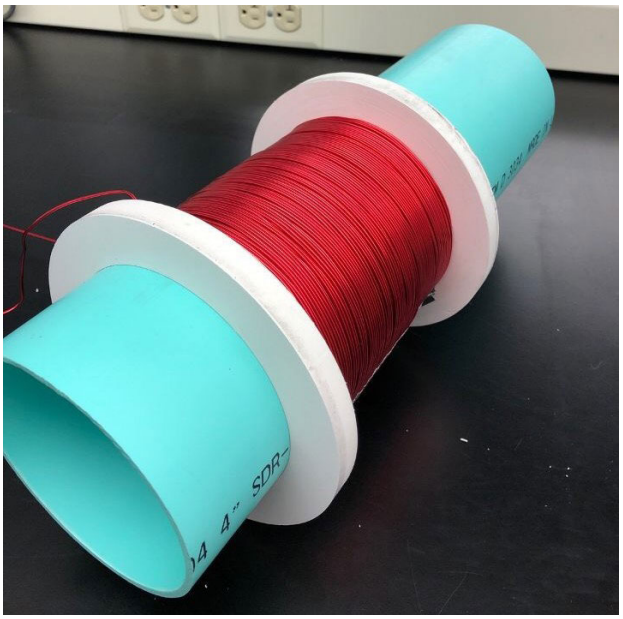

FIGURE 15. Preliminary coil prototype.

This coil is 5 inches in length and consists of 200 turns of wire, this was connected to the charging circuit which contained 10 capacitors as a discharging source. Upon preliminary verification of the coil it was found that while it did create a magnetic field, the intensity of the field was dispersed over the full 5 inches of the coil, meaning that the instantaneous force on any object placed within the coil was greatly lessened. Because the system relies on a strong instantaneous force, this had to be improved, so the coil design was altered. First the length was shortened from 5 inches to 3 inches, and then the number of turns was doubled from 200 to 400. This redesign is shown in the following figure:

A revised circuit was also implemented after the coil was altered in order to maximize the magnetic field generation within the coil. The only change made was to the power source and the capacitor banks. The 50VDC rated capacitors were switched out for 100VDC rated capacitors of the same capacitance value. The power supply was also changed to a battery system that could charge the capacitor bank to a much higher voltage of 100 volts. As shown in equation 4,

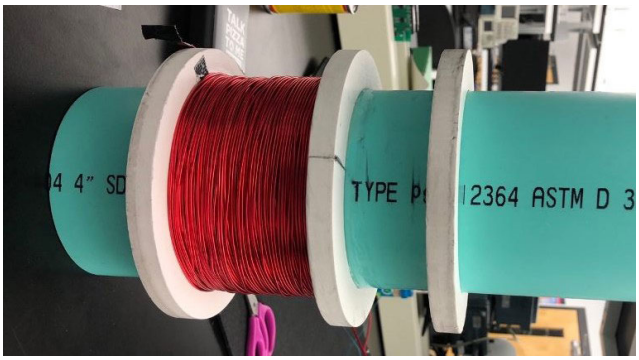

FIGURE 16. Revised coil prototype.

increasing the voltage over these capacitors and keeping the same capacitance greatly increases the current discharging from the capacitor bank. Therefore a much stronger magnetic field is created without altering any other aspects of the circuit. Also because the relay is rated to 100V, no changes had to be made to the switching apparatus. All following tests ran on the system were completed with this circuit configuration.

Before testing this system physically, simulations were ran on the new circuit and coil configuration. Recalculating inductance using equation 5 results in an inductance of .0334 henries. This was then combined with a new capacitor charge voltage of 100V. While this new coil size would greatly increase the concentration of the magnetic field; the increased inductance not only cuts down on the maximum current magnitude but would also greatly increase the pulse width. This relation is shown in equation 4 for maximum current. When the circuit simulations were rerun, the following result was observed:

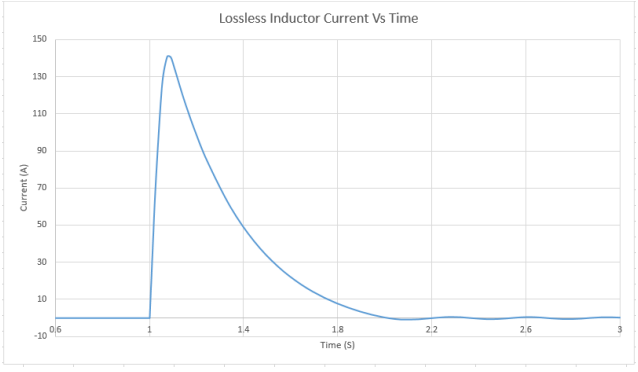

FIGURE 17. Simulation result of lossless circuit.

As shown above, this results in an extremely high current peak of 140 amperes, but the pulse width has increased tenfold, and is now roughly equivalent to one full second. A pulse width of this length would surely lead to an unwanted oscillation in the armature, lessening the overall power of the device. Ordinarily this would be a large problem with the design, but there is one aspect of the simulation that can be altered to fix this. The simulations used until this point assume a lossless coil. In reality there is discernible loss due

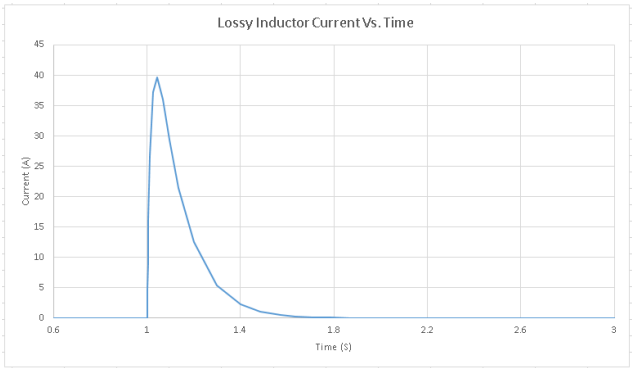

FIGURE 18. Simulation result of lossy circuit.

to the internal resistance of of the wire over. This combined with the 400 turns over a diameter of 5 inches means there is over 200 feet of wire used within the coil. Upon measuring the resistance of the coil, it was found to be 2.5 ohms. This cannot be ignored for a realistic simulation, but it is also better for the system to be modeled with resistance because a series resistance with the inductor will greatly cut down on the pulse width. Unfortunately, this decreases the initial current spike, but was necessary to keep in the model for real world accuracy. Using this resistance in a now lossy simulation, the following result is derived for lossy inductor current.

In the new lossy simulation denoted above, the internal resistance of the wire cuts down on the pulse width considerably, reducing it to roughly 0.4 seconds. It was decided that the pulse width of 0.4 seconds would be acceptable, due to the fact that the armature moves slower in water than in air. Equally as important the maximum current has been reduced from 140 amperes to roughly 40 amperes. While this may not be the most desirable result, it is the most realistic model of the system and the increased coil turns and decreased length will lead to a stronger magnetic field despite the reduced current. This result of 40 amperes peak was then ported into ANSYS Maxwell for magnetic field simulation, and run with the same parameters as earlier:

The new simulations confirm the field's strength was increased as a result of both shortening the coil and increasing the number of turns. The maximum strength of the magnetic field was increased to 0.37 teslas, almost doubling the original coil's output. The average field around the armature was found to be 0.15 teslas, which was then plugged into equation 3 to calculate the new force on the armature. This new value was found to be 17.85 newtons. The higher amount of force will be able to expel the payload at roughly 2X the initial velocity, greatly improving the overall system.

Simple verification with the charging circuit showed this created a much stronger concentrated field that was able to provide a much higher instantaneous force. When ferromagnetic metals were placed inside the tube a much faster movement was observed, and the tube was able to even launch the armature sleds out of the tube. When early UUV prototypes were placed in the tube, they were easily able to clear the end of the tube in dry experiments. In order to compare real world

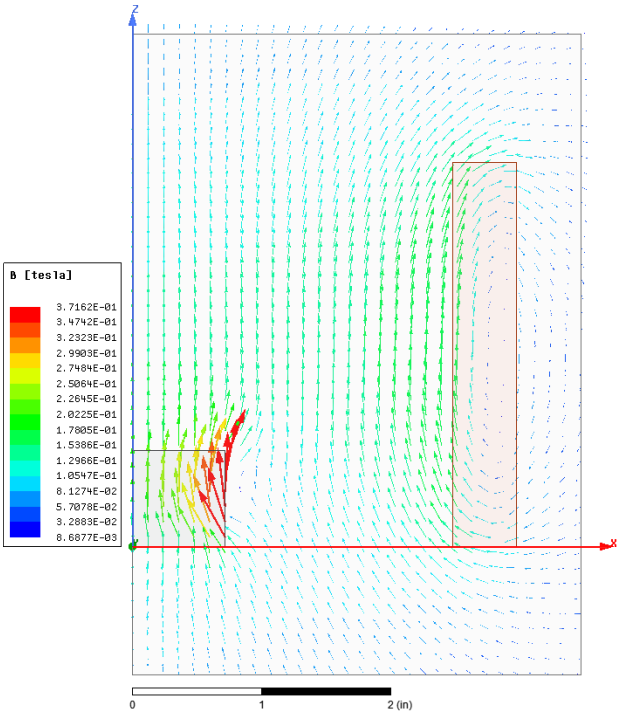

FIGURE 19. Simulation result of updated launcher design.

results against the simulations, an oscilloscope with a capture feature was used to record the voltage across the coil during the discharging phase of the circuit. This experimental result is shown below:

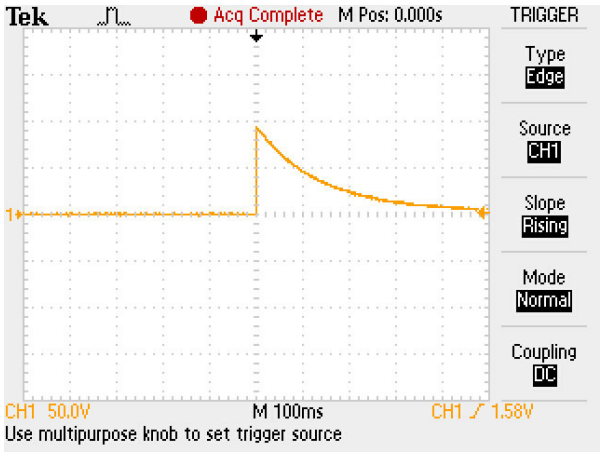

FIGURE 20. Experimental coil voltage vs time.

As shown here, the full energy of the capacitor bank is transferred to the coil almost instantly as the firing switch is toggled. The pulse seen here is also shorter than the simulated firing, with the capacitors almost fully discharged by 300ms. It is reasonable to assume that the current lags the voltage slightly due to this being an RLC circuit, so the current pulse is likely to be a little longer than the voltage pulse shown. With the voltage at roughly 100V and the resistance at 2.5 ohms, the peak current in the inductor is

then simply 40 amperes. This directly matches the simulation result shown in figure 18, and proves a very viable simulation model. This coil and circuit iteration was further tested physically by placing an armature sled within the tube and attaching it to a spring gauge. When this test was completed it was found that the sled could easily transfer nearly 2 foot pounds of force to an object within the tube. This correlates to almost 9 newtons directly transferred to the projectile at a considerable velocity. With these parameters of the system fully tested and specified, the most effective armature design shall now be discussed.

A. SKI ARMATURE

Within this coil, the first armature design is contained. This design consists of a solid sled of stainless steel connected through springs and screws to 3 rubber skis that slide down the inner walls of the tube. A rear view of this constructed armature is shown below:

FIGURE 21. Constructed ski armature prototype.

When this armature was initially constructed it was found that the springs were stronger than expected, and this resulted in the rubber skis being pressed against the inner walls of the tube with a sizeable force. It was also noted that the rubber skis themselves were made of a material that gripped the PVC walls of the tube. The sled shown in the middle of figure 16 was also over an inch thick of solid steel, contributing to a heavy weight for the magnetic field to move. Steel is an alloy made of multiple metals, and is not as magnetic as other metals like iron. Thus the magnetic field would have less of an effect on this sled due to its low magnetic permeability. All of these factors combined led to fairly low expectations for this armature in the testing phases.

For the dry testing, it was clearly visible that this armature would be rather difficult to move due to the reasons discussed above. When the current pulse was applied to the coil, the armature moved forward in the tube, but at a low velocity and not over a very long distance, merely 5 inches. The armature was able to push the projectile, but it would not clear the tube without hitting the bottom the edge. This design was promising was determined to be unsuccessful, so further testing was abandoned in favor of another design.

B. WHEEL ARMATURE

The second, and ultimately chosen design for the armature is very similar to the first, but with wheels attached to the sled instead of rubber skis. The wheels would be aligned with a track system on the interior of the tube. Theoretically this design would have significantly less friction than the ski design, because of the use of rolling wheels instead of the static rubber skis. Thus, in theory, this design would be able to transfer more energy into the projectile from the armature. The wheel and rail system would also have a negligible effect on the drag force within the tube, making it a clear option for a final design. A 3D model of the wheeled armature design is shown below:

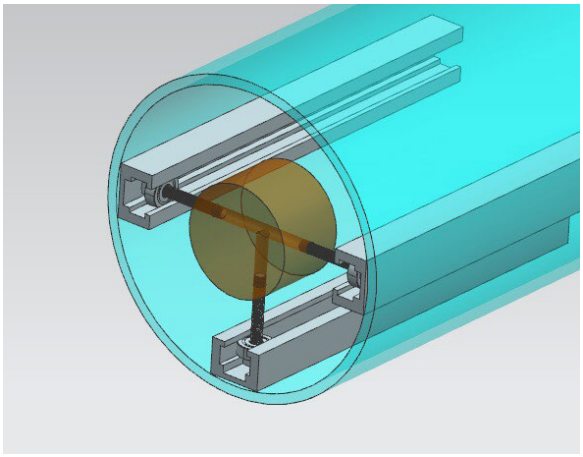

FIGURE 22. Wheel armature 3D model.

This concept relies on the three wheels shown, attached via screws to the sled. While the model above shows a third wheel connected to the bottom side of the armature, the physical unit incorporates a ball bearing slide mechanism similar to those used in common desk drawers. This provides support for the armature to rest on and moves much more easily down the tube than a horizontal wheel through a track would. The first iteration of this system used steel tracks. When the coil received an impulse of current, the armature did not move. This was a result of the steel tracks shielding the armature from the magnetic field, allowing no energy to push it down the tube. The second iteration of the track armature utilized aluminum tracks instead, as it was found that the magnetic permeability of aluminum should not affect the field as much as steel. An ANSYS simulation was performed to check the worst case scenario for an aluminum track, with the results shown below:

As the model shows, the average field around the armature weakens to about 0.13 teslas. This is a small reduction of about 0.02 teslas from the model without aluminum tracks. This reduces the force on the armature to 13.14 newtons, which is a reduction of 4.44 newtons. This is a very

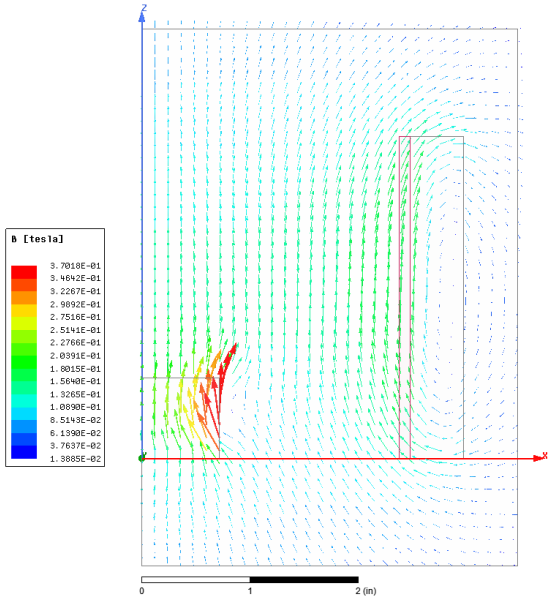

FIGURE 23. Track armature 2D model with aluminum tracks.

significant drop in force, and was experienced in the dry testing as a much slower and weaker armature movement was observed.

To avoid this in future testing, 3D printed tracks were made to stabilize the armature, along with an aluminum ball bearing bottom rail to minimize losses. The 3D printed side rails and aluminum slide all had roughly the same level of friction as the steel rails and were significantly lighter, making them the obvious design choice. This completed physical design is shown in the following figure:

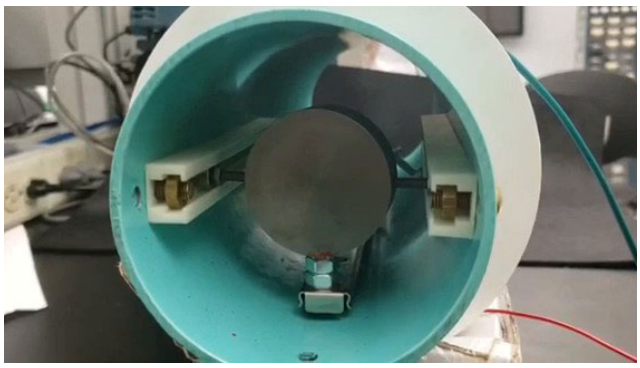

FIGURE 24. Wheel armature with 3D printed tracks and aluminum slide.

This new rail and wheel system was then tested in a dry environment. It was found that the physical system with the updated rails functioned exactly as expected, providing a significantly higher force to the projectile within the tube. It was observed that in air the armature moved with such force that its wheels bounced back off of the screws at the end of the rails and almost returned to its original firing position. Therefore this design was chosen for the final wet-testing.

C. WET-TESTING

Wet testing was completed on the system exclusively with the wheel and track armature specified above. Before the launcher was tested underwater it first had to be waterproofed, which was done by sealing the coil with a larger diameter PVC pipe, and running the wires through a perpendicular tube up through the surface of the tank. This follows the proposed waterproofing design shown in figure 13. This now waterproofed coil was then placed in the testing tank and several gallons of water were added to submerge it. In order to measure the exit velocity, a white backdrop with 1 inch spaced lines was placed at the end of the tube. A high speed underwater camera was then mounted on the opposite side of the tank in order to record the UUV against the specified background. Thus by observing how many lines the UUV travels across over a certain time period, the approximate exit velocity could simply be derived as the distance over time. The complete tank testing rig is shown below:

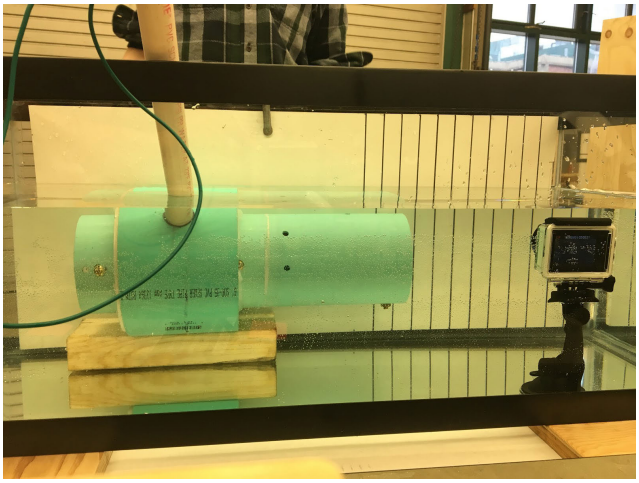

FIGURE 25. Underwater coil testing rig.

It should be noted that this rig was constructed with a tank full of ordinary tap water with negligible salinity, although theoretically the salinity of the water should not have an effect on the creation of the magnetic field. The testing tank shown is 3 feet long by 1 foot wide. This allows enough space within the tank for the projectile to fully exit the tube and travel roughly one foot once the tube has been completely cleared. This was deemed safe for testing due to the expected force on the projectile not being enough to cause it to break the glass. This specific testing rig was used to obtain all of the experimental results discussed herein.

The first underwater test launches were performed with a cylindrical, non-buoyant PVC pipe which was approximately eight inches in length and one inch in diameter. This was a makeshift projectile stuffed with buoyant material and no caps on either end. During trials with this projectile, the system was able to achieve an average velocity of 1.9 feet per second. This velocity was calculated by taking the reference frames in the time line of the captured video, with

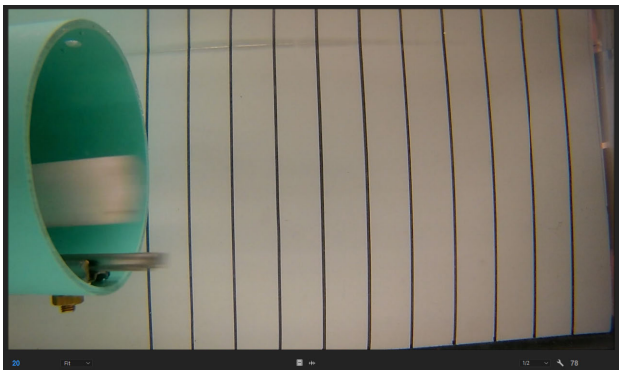

FIGURE 26. Initial reference frame of test launch.

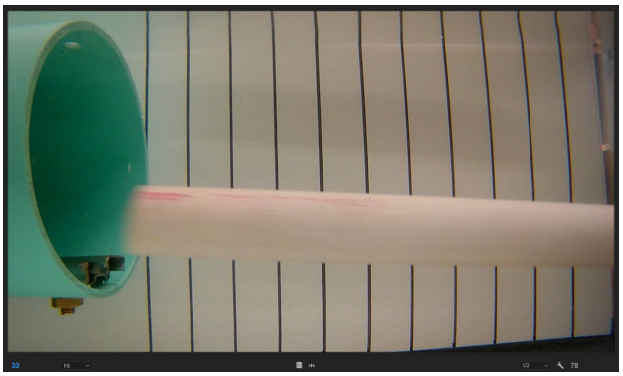

FIGURE 27. Final reference frame of test launch.

the first being the frame the UUV begins to move, and the last frame in which the back end of the projectile reaches the initial starting point. The length of the UUV is divided by the number of frames in between these moments, and then multiplied by 30 frames per second to get the velocity in inches per second. This is then divided by 12 to get the value in feet per second.

But after initial testing and calculation, the results were inconsistent in both speed and path of motion. This was due to the nature of the test projectile and the tube. The pipe was not neutrally buoyant, so it dragged along the bottom of the outer tube, and it was not supported like the final design. This created inconsistencies as the projectile was not centered on the armature, which means with the final UUV design, the test results should be qualitatively more accurate and consistent. Even with these drawbacks the launcher was still able to expel this makeshift projectile fully from the tube. This was a promising initial result and verified the launcher operation. The reference frames from the test launch video taken and compared to calculate the average velocity are seen below in figures 26 and 27. The first frame is the exact second that the payload reaches the edge of the outer tube, and the second frame is the exact second that the payload fully clears the outer tube. The camera recorded video of this experiment at 60 frames per second, enabling such an exact selection of reference frames:

With this initial testing successfully completed, it was now necessary to house the electronics in a safe, watertight case to protect them from any splashes. For the circuit components a housing unit of high quality, fire retardant ABS plastic was selected. This container also utilizes a silicone rubber gasket to prevent any possible moisture from entering and disrupting the circuit components. The operating switches, as well as an in-line voltage meter to monitor capacitor voltage were all mounted on the top of the housing for practical usage and circuit monitoring. This final enclosure with operator controls is shown below:

FIGURE 28. Circuit housing external assembly.

The internal view of the circuit box is shown below in figure 29. An enclosure with spare area inside was selected so that extra components could be added during testing. These components include a third capacitor bank, and room for more batteries. The 12V battery shown is used to provide the bias to activate the relay in the charging circuit, and the only other components housed inside the box are the capacitor and the 9V battery banks. Wires were organized with cable ties to prevent any kind of unexpected shorting to occur and to make debugging easier in the event of a failure.

A quick round of testing showed the circuit functioned exactly as designed within this new housing. Thus all components were sufficiently waterproofed and organized, so the final round of wet testing for the system was implemented.

The second round of wet testing was completed with the experimental setup shown in figure 25. The camera was set to record at 60 frames per second, and slowed down to obtain a clear traveling distance within a certain time frame. This test was performed with an improved UUV prototype which was slightly non-buoyant, approximately 2'' in diameter and 10'' long. This UUV was significantly larger than the model tested earlier in this report, and sunk at a slow rate within the water. This UUV was not only thicker, but longer than the makeshift UUV tested earlier. This projectile was found to have an average velocity of 1.1 feet per second as it exited the outer tube. The reference frames for this test can be seen below in figures 30 and 31. These reference frames were measured slightly differently; the first frame was taken as the payload exited the tube, at the third black line marker. The second frame was as the payload reached the final black marker visible to the camera lens. With this range, an accurate average velocity could be calculated for the entire duration of the launch.

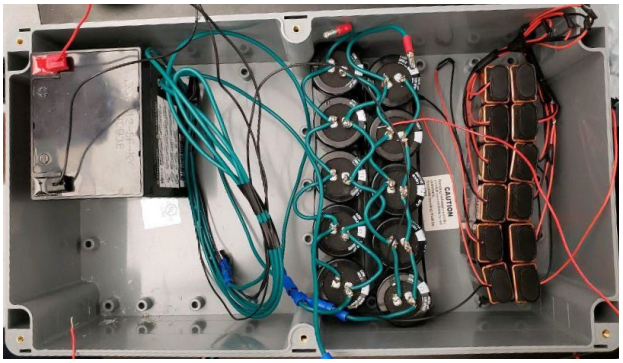

FIGURE 29. Circuit housing internal assembly.

FIGURE 30. Initial reference frame of final test launch.

FIGURE 31. Final reference frame of final test launch.

Thus the final round of wet testing could be deemed successful. As shown in figures 30 and 31, the projectile is able to fully clear the tube, and travel some distance before sinking. This satisfies the system requirements outlined in section 2 of this report. This apparatus was tested several times to ensure the functionality of the system, and the payload did not fail to clear the tube in a single trial of the experiment.

With this stage of testing completed within the time allotted, there was an opportunity to test a new outer tube material as well, but on a small scale. A miniature, titanium tube launcher was constructed to test whether or not the material would work without shielding the magnetic field generated by the coil. This construction can be seen below:

Tested with a small iron projectile, the design is capable of launching the object with a high initial velocity, thus it can be

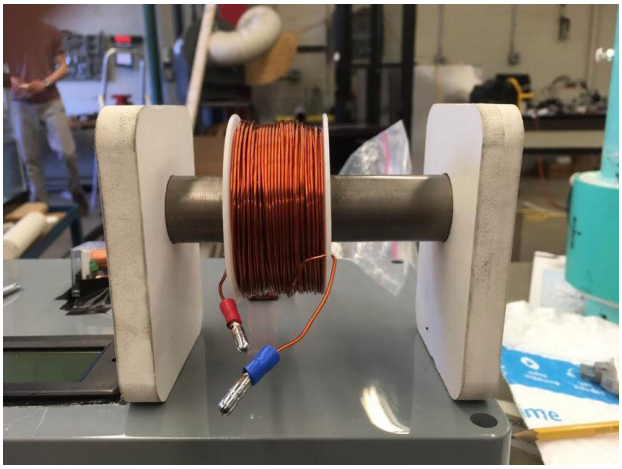

FIGURE 32. Test prototype with titanium outer tube.

determined that it would be scalable to the current prototype size. Therefore, a launcher made of titanium, or another metal with low magnetic permeability would be functional. This is important as while the PVC launcher is capable of successful launches, the structural integrity of the material would be significantly less than the same design manufactured with metal instead. In a submarine, or other underwater vehicle, it is crucial for the launcher to withstand immense forces, so this finding is important to the viability of the design.

VII. CONCLUSION

With testing completed, it can be concluded that electromagnetic propulsion is viable underwater and is scalable. The UUV is able to clear the tube without dragging, and exits at the high velocity needed for expulsion. Several setbacks were addressed throughout the duration of the project. One was the initial coil design. It was too weak to launch the armature with the sled scheme, but this was overcome with the final, shorter design with more coils. The second important setback was the failure of the sled armature, as it failed to move with a considerable velocity even with the improved coil design. The track and rail system for the armature came about as a result of this issue, which lead to the final build of the launcher used to complete the project.

With the successful underwater tests, all deliverables were met. For further study, different material choices for the launcher outer tube could be explored, along with testing out the other electromagnetic launch schemes, such as the railgun design. Other design considerations that could be explored could be utilizing higher voltage capacitors, or multiple stages of coil to increase the launch strength. This research also create opportunities to test performance as a projectile launcher in other mediums such as in vacuum.

APPENDIX

DERIVATION OF EQUATION 5

To begin the derivation, first consider the energy stored in the capacitor bank at the beginning of the discharge cycle, given

by the following equation:

$$E = \frac{1}{2}CV^2$$

Now this equation can be equated to the maximum energy that the inductor can store, if it is assumed that the capacitor transfers all of its stored energy into the inductor as the circuit is switched to firing mode.

$$\frac{1}{2}CV^2 = \frac{1}{2}LI^2$$

Now through algebra the equation can be manipulated to solve for the current passing through the inductor.

$$I = \sqrt{\frac{CV^2}{L}}$$

Which is equivalent to equation 5 if the charge of the capacitor is substituted in as Q.

ACKNOWLEDGMENT

This research was mentored by Naval Sea Systems Command, especially Dr. James M. LeBlanc, Michael E. Sheahan, and Robert G. Gregory. The authors would also like to thank Menna Elfouly, Austin Gallimore, and Liam Perkins from UConn Senior Design Mechanical Engineering team ME28 for their contributions in research, design, and construction of the final prototype.

REFERENCES

[1] L. John, "Water balloon's shoots weapons in future launching system," *Undersea Warfare*, vol. 3, pp. 83–85, 1999.
[2] M. R. Doyle, D. J. Samuel, T. Conway, and R. R. Klimowski, "Electromagnetic aircraft launch system-EMALS," *IEEE Trans. Magn.*, vol. 31, no. 1, pp. 528–533, Jan. 1995.
[3] D. Patterson, A. Monti, C. Brice, R. Dougal, R. Pettus, D. Srinivas, K. Dilipchandra, and T. Bertoncelli, "Design and simulation of an electromagnetic aircraft launch system," in *Proc. IEEE Ind. Appl. Conf., 37th IAS Annu. Meeting*, vol. 3, Oct. 2002, pp. 1950–1957.
[4] D. Cébron, S. Viroulet, J. Vidal, J.-P. Masson, and P. Viroulet, "Experimental and theoretical study of magnetohydrodynamic ship models," *PLoS ONE*, vol. 12, no. 6, Jun. 2017, Art. no. e0178599.
[5] D. Normile and R. Langreth, "Superconductivity Goes to sea," *Pop. Sci*, vol. 241, no. 5, p. 80, 1992.
[6] T. Lin, J. Gilbert, and R. Kossowsky, "Sea-water magnetohydrodynamic propulsion for next-generation undersea vehicles," Appl. Res. Lab., Pennsylvania State Univ., State College, PA, USA, Tech. Rep. AD-A218-318, 1990.
[7] O. M. Al-Habahbeh, M. Al-Saqqa, M. Safi, and T. A. Khater, "Review of magnetohydrodynamic pump applications," *Alexandria Eng. J.*, vol. 55, no. 2, pp. 1347–1358, Jun. 2016.
[8] V. Geiger, "System for launching an underwater vehicle," EP Patent 2 530 423 A1, Jan. 15, 2014.
[9] J. C. Meng, "Superconducting electromagnetic torpedo launcher," U.S. Patent 5 284 106, Feb. 8, 1994.
[10] C. E. Galliano, "Rotary electromagnetic launch tube," U.S. Patent 6 854 409, Feb. 15, 2005.
[11] H. Matsui, "Launching apparatus for underwater payload," U.S. Patent 15 177 537, Dec. 22, 2016.
[12] E. T. Laskaris and M. V. Chari, "Electromagnetic launcher," U.S. Patent 4 971 949, Nov. 20, 1990.
[13] Z. Zabar, "Apparatus for driving a coil launcher," U.S. Patent 4 926 741, May 22, 1990.
[14] R. S. Hawke, J. K. Scudder, and K. Aaland, "Multiple stage railgun," U.S. Patent 4 343 223, Aug. 10, 1982.
[15] L. J. Jasper Jr, "Electromagnetic railgun with a non-explosive magnetic flux compression generator," Jun. 28, 1988, U.S. Patent 4 753 153.
[16] W. H. Kurherr, "Electromagnetic projectile accelerator," U.S. Patent 4 432 333, Feb. 21, 1984.
[17] A. Sitzman, D. Surls, and J. Mallick, "Design, construction, and testing of an inductive pulsed-power supply for a small railgun," *IEEE Trans. Magn.*, vol. 43, no. 1, pp. 270–274, Jan. 2007.
[18] A. Pokryvailo, M. Kanter, Z. Kaplan, and V. Maron, "Design and testing of a 5 MW battery-based inductive power supply," *IEEE Trans. Plasma Sci.*, vol. 26, no. 5, pp. 1444–1453, Oct. 1998.
[19] S. Kakinuma, "Waterproofing device for control circuit used in outboard engines," U.S. Patent 5 053 634, Oct. 1, 1991.
[20] M. Kondo, "Waterproofing apparatus for terminal connecting portion of sheathed wire," U.S. Patent 6 761 551, Jul. 13, 2004.

CHRISTIAN CORWEL was born in Bridgeport, CT, USA, in 1997. He enrolled at the University of Connecticut, in Fall 2015.He received the B.S. degree in electrical engineering, in May 2019. He is currently an Aerospace Components Engineer with the United Technologies Corporation.

GEORGE ZOGHBI was born in Windham, CT, USA, in 1996. He began studying at the University of Connecticut, in Fall 2014. He received the B.S. degree in electrical engineering, in May 2019. He is currently an Electrical Engineer with Diversified Technologies, Inc.

STEVAN WEBB was born in Morristown, NJ, USA, in 1995. He enrolled at the University of Connecticut, in Fall 2014. He received the B.S. degree in electrical engineering, in May 2019. He is currently a Systems Engineer with General Dynamics Electric Boat.

ABHISHEK DUTTA (Member, IEEE) received the M.Sc. degree from the University of Edinburgh and the Ph.D. degree from Ghent University. He is currently an Assistant Professor of electrical and computer engineering and biomedical engineering with the United Technologies Corporation–Institute of Advanced Systems Engineering and the Connecticut Institute of Brain and Cognitive Sciences. He holds a postdoctoral position at the University of Illinois at Urbana–Champaign.